



Detection of glucose in synthetic tear fluid using dually functionalized gold nanoparticles

S. Manju, K. Sreenivasan*

Biomedical Technology Wing, Sree Chitra Tirunal Institute for Medical Sciences & Technology, Poojapura, Trivandrum 695012, India

ARTICLE INFO

Article history:

Received 16 April 2011

Received in revised form 16 August 2011

Accepted 16 August 2011

Available online 22 August 2011

Keywords:

Gold nanoparticles

Aminophenyl boronic acid

Rhodamine B isothiocyanate

Synthetic tear fluid

Fluorescence

ABSTRACT

A simple fluorescent sensing of glucose in aqueous fluids (e.g. tear fluid) using dually functionalized gold nanoparticles is presented. As a first step gold nanoparticles (AuNPs) were synthesized using oxidised dextran which acted both as reducing and stabilizing agent. Aminophenyl boronic acid was conjugated onto AuNPs by Schiff's base formation and the formed Schiff's base was stabilized by sodium borohydride reduction. Rhodamine B isothiocyanate (RBITC) was then assembled onto the modified AuNPs. The fluorescence of RBITC was nearly quenched and found to be revived when glucose was added. It is reasoned that the glucose binding induces restructuring of the surface assembly resulting in an overall increase in the size and thereby enhancing the distance between the gold core and fluorophore. TEM image and size measurements using dynamic light scattering (DLS) in fact, reflected this possibility. The increase in fluorescence was proportional with the concentration of glucose enabling quantitative detection. A good linearity was observed between the fluorescence intensity and glucose concentration in a range of 0.025–0.125 μM with detection limit of $0.005 \pm 0.002 \mu\text{M}$. The potential of the method was demonstrated by measuring glucose in real tear fluids collected from volunteers. The method is extremely sensitive and can be employed to measure low concentration of glucose in aqueous fluids such as tear.

© 2011 Elsevier B.V. All rights reserved.

1. Introduction

Diabetes is a chronic disease that occurs either when the pancreas does not produce enough insulin or when the body cannot effectively use the insulin. Hyperglycaemia, or elevated blood sugar, is a common effect of uncontrolled diabetes. Uncontrolled diabetes leads to serious health disorders including cardiovascular disease, kidney failure and blindness. One of the major challenges in the management of diabetes is the monitoring of glucose concentrations. Blood glucose monitoring is required in regulating frequency of meals, activities, and schedule of medications [1–7]. Despite extensive efforts, no simple method is currently available for the continuous non-invasive monitoring of blood glucose. The measurement of glucose levels in readily available body fluids, such as tears, may have the potential benefit of eliminating the finger-stick test (the current standard method used) and increase compliance with glucose monitoring among diabetic patients [8–10]. The glucose concentration in tears is known to correlate with the blood glucose concentration. Lane et al. [8] compared tear glucose dynamic differences between diabetic and nondiabetic patients after the administration of carbohydrate load. In their study, positive correlations was found between the levels

of blood and tear glucose. Thus an estimation of tear glucose may be employed as an effective method for detecting and monitoring of diabetes mellitus. So far several methods have been proposed for sensing glucose in tear fluid. For example Badugu et al. have shown contact lens-based sensing devices for monitoring the concentration of glucose in tears [11]. Taormina et al. have reported the use electron spray ionization mass spectrometry for the detection and estimation glucose in tear fluid [12].

Metallic nanoparticles such as gold and silver are extensively studied for the noninvasive detection of low levels of glucose [13–16]. These methods are based on the Concanavalin A immobilized nanoparticles. The versatile chemistry available for surface functionalization of AuNPs makes it suitable for sensing a vast number of analytes [17–19]. AuNPs show plasmon absorption in the visible region depending upon their size and shape. The position of this band can be affected by changes in the dielectric constant in the vicinity of the particle, and this property has been exploited for sensing applications [20]. Aslan et al. [13] demonstrated the dextran coated AuNPs aggregated by the controlled addition of Concanavalin A as a sensing approach for glucose. Modification of AuNPs with fluorophores is an alternate method for the development of biosensors as well as optoelectronic devices. Resonant energy transfer (RET) systems consisting of organic dye molecules and AuNPs have recently gained considerable interest in biphotonics as well as in material science [21–24]. The variation of optical features of metal clusters in the presence and absence of specific

* Corresponding author. Tel.: +91 471 2520248; fax: +91 471 2341814.

E-mail addresses: sreenisct@yahoo.co.in, sreeni@sctimst.ac.in (K. Sreenivasan).

analytes has been explored as a sensitive route for the detection and estimation of those analytes. Several examples of excited state quenching by AuNPs have been reported [25,26]. In one of the study Huang and Murray have described the quenching of small dyes molecule by AuNPs [27]. In another study Dubertret et al. [28] have demonstrated AuNPs as an effective proximal quencher in DNA molecular beacons. However, glucose modulated emission properties of AuNPs functionalized with a fluorophore and glucose selective ligand as an approach for the sensing of glucose in aqueous fluids has not been reported. Here in, we report one step process for the generation of dextran coated AuNPs (Dex@AuNPs) and further conjugation of aminophenyl boronic acid to Dex@AuNPs through Schiff's base formation. Rhodamine B isothiocyanate (RBITC) was adsorbed onto the aminophenyl boronic acid functionalized AuNPs (ABA@AuNPs). The fluorescence of RBITC@AuNPs was quenched to a considerable extent. The fluorescence was however, revived and found to increase proportionally with the concentration of glucose. This observation has prompted us to use RBITC@AuNPs for the detection and quantification of glucose in synthetic and real tear fluids.

2. Experimental

2.1.1. Materials

Chloroauric acid ($\text{HAuCl}_4 \cdot 3\text{H}_2\text{O}$), dextran from *Leuconostoc mesenteroides* (average molecular weight 64,000–76,000), sodium periodate (NaIO_4), 3-aminophenyl boronic acid-hemisulfate salt $\geq 95\%$ (ABA), Rhodamine B isothiocyanate (RBITC), sodium borohydride, sodium bicarbonate and α -D-glucose anhydrous 96% were obtained from Sigma–Aldrich, Bangalore, India. Lubricant eye drops, 0.5% w/v (Synthetic tear fluid), were obtained from Promed Exports Pvt. Ltd, India. These chemicals were used as received. Other analytical grade solvents were purchased from Merck Mumbai, India. Ultrapure water (18.2 mV resistivity) was obtained from a Milli-Q water purification system. Deionized water (DW) is used throughout the experiments.

2.1.2. Characterization of functionalized AuNPs

A Nicolet 5700 FTIR spectrophotometer (Madison, USA) was used for recording the infrared spectra of the modified AuNPs. The spectra were recorded in the range of 4000–400 cm^{-1} . The samples were dried and was mixed with KBr and made into pellets. UV-VIS Spectroscopy was performed on UV-Visible spectrophotometer (Cary model 100 Bio, Melbourne, Australia) using 1 cm Quartz cuvette. Spectra were collected within a range of 400–800 nm. The fluorescence spectra were collected using a Cary Eclipse model EL 0507 spectrofluorimeter (Melbourne, Australia). Particle size distribution of the nanoparticles was determined using Photon correlation spectroscopy on DLS instrument (MalvernQ2 Zetasizer Nano ZS, UK) with a He–Ne laser beam at a wavelength of 633.8 nm. Zeta potential (ζ) values were obtained using the same instrument by applying an electric field across the dispersion. Transmission electron microscopy (HITACHI, H-7650, Tokyo, Japan) was also employed to visualize the AuNPs after each functionalization steps. Samples were prepared by depositing one drop of colloidal solution of AuNPs in water on a copper grid with formvar film and air-dried at room temperature.

2.1.3. Periodate oxidation of dextran

Periodate oxidation of dextran to generate –CHO groups are well known [29]. We adopted this method for the preparation of dextran dialdehyde. Briefly, 5 g of dextran (0.031 M) was dissolved in 90 mL distilled water taken in a 250 mL round bottom flask. To this 3.03 g

(0.0155 M) sodium periodate dissolved in 10 mL distilled water was added and stirred magnetically in dark at 25 °C for 6 h. This reaction conditions are known to produce around 25% oxidation in dextran [30]. The reaction mixture was then dialyzed against distilled water using dialysis membrane (molecular-weight cut off (MWCO) 3500 Da) till the dialyzate was periodate free. Periodate diffusion into distilled water was checked using dilute silver nitrate solution. When the presence of periodate was no longer detectable, dialyzate was freeze dried and oxidized dextran was collected.

2.1.4. Synthesis of AuNPs using oxidised dextran

To 50 mL of 2 mM aqueous solution (34 mg activated dextran in 100 mL deionised water) of activated dextran added with 500 μL of 10^{-2} M HAuCl_4 . The reaction mixture was allowed to boil until it turned red, indicating the formation of AuNPs in the solution. Then, the solution was cooled to room temperature and used as such for further modification. The formed particles were abbreviated as Dex@AuNPs.

2.1.5. Chemisorption of aminophenyl boronic acid on the surface of Dex@AuNPs

We modified AuNPs surfaces with boronic acid moieties, which can form reversible covalent bond with glucose molecule. Aminophenyl boronic acid (ABA) was conjugated on the Dex@AuNPs surface by Schiff base formation between amino group of ABA and the aldehyde group in the activated dextran. Briefly, 10 mL of Dex@AuNPs were gently mixed with 2 mL of 0.01 M aminophenyl boronic acid in sodium bicarbonate buffer (0.5 mM) and 100 μL of 5 mg/mL sodium borohydride in 0.05 M sodium bicarbonate buffer. The reaction mixture was placed in the orbital shaker at 37 °C for 4 h at 200 rpm. After 4 h of reaction, untreated excess reagent were removed by dialysis using dialysis membrane (MWCO 3500 Da) against deionized water to get aminophenyl boronic acid conjugated AuNPs (ABA@AuNPs).

2.1.6. Adsorption of Rhodamine B isothiocyanate on ABA@AuNPs

RBITC was strongly adsorbed on ABA@AuNPs by simple hydrogen bonding. Briefly, 5 mL of the above colloidal suspension (ABA@AuNPs) were mixed with 0.5×10^{-3} M L^{-1} , 10 μL RBITC solution and kept in an orbital shaker overnight in dark at 200 rpm and at 25 °C. The reaction mixture was then dialyzed against deionized water, in the dark, to remove free RBITC.

2.1.7. Fluorescence detection of glucose using RBITC@AuNPs

Fluorescence spectra were recorded on a Cary Eclipse model EL 0507 sepectrofluorimeter at room temperature ($\sim 25^\circ\text{C}$). The fluorescence spectrum of free RBITC and the RBITC@AuNPs were recorded separately in aqueous solutions of synthetic tear fluid at pH 7.4. Glucose solution was prepared in 10% of synthetic tear fluid and the pH was adjusted to 7.4. For each measurement 0.5 mL of the RBITC@AuNPs solution (pH 7.4) was taken and added different concentration of glucose (e.g. 0.0025 μM , 0.0055 μM , 0.008 μM , 0.011 μM , 0.0139 μM , 0.028 μM , 0.042 μM , 0.055 μM , 0.0694 μM , 0.083 μM , 0.0972 μM , 0.11 μM , 0.125 μM , 0.138 μM , 0.152 μM) and the spectrum was generated in each case. The fluorescence intensity was corrected for dilution.

2.1.8. Detection of glucose in real tear fluid using RBITC@AuNPs

Tear fluids were collected from five female volunteers (age 25–30 years by slightly activating the eyes using onion. 500 μL of RBITC@AuNPs solution was incubated at room temperature for

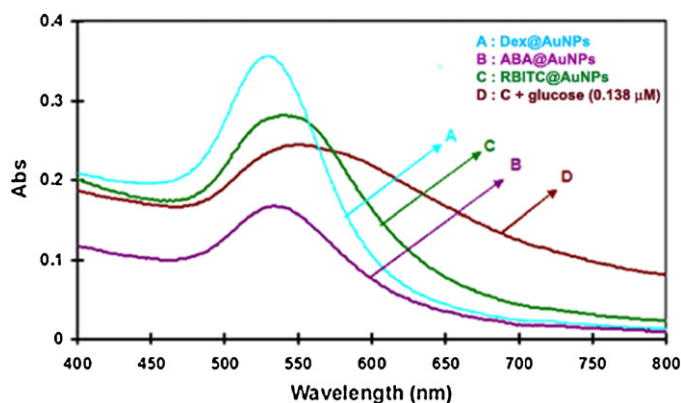


Fig. 1. Plasmon absorption spectra of (A) Dex@AuNPs, (B) ABA@AuNPs, (C) RBITC@AuNPs and (D) in the presence of glucose (0.138 μ M).

10 min with 20 μ L each of tear collected. Fluorescence spectra were then collected.

3. Results and discussion

Periodate oxidation of dextran at room temperature cleaves the vicinal glycols to form activated or oxidized dextran (Scheme 1). Periodate oxidation of dextran in dilute aqueous solution initially proceeds in a random manner and is usually accompanied by extensive cleavage of the chain. In this work we limited percentage oxidation to 25% by taking half the mol equivalent of periodate to that of dextran [30]. Since dextran dialdehydes are studied extensively, we did not follow further characterization of these entities. Dex@AuNPs was synthesized by one step process by boiling an aqueous solution containing chloroauric acid (HAuCl_4) and activated dextran. The solution turned red within 30 min and exhibited the characteristic plasmon absorption peak around 530 nm, indicating the formation of AuNPs. The role of dextran as a reducing agent instead of citrate in the synthesis of AuNPs has been demonstrated [31,32]. Dextran plays the dual role of a reductant and a stabilizing agent of the generated AuNPs. Dex@AuNPs was used without further purification. Dex@AuNPs was stable up to 1 month at 4 $^{\circ}\text{C}$.

Changes in the plasmon resonance absorption were monitored during each stages of modification. The absorptions peaks of the particles are shown in Fig. 1. The Dex@AuNPs exhibited surface plasmon resonance (SPR) absorption at 530 nm indicating that the particles were not aggregated but dispersed as individual particles. Dex@AuNPs modified with aminophenyl boronic acid (ABA@AuNPs) exhibited a plasmon peak around 536 nm. The red shift in the plasmon peak is produced by the perturbation in

Table 1

ζ potential of AuNPs in aqueous solution as a function of surface modifications.

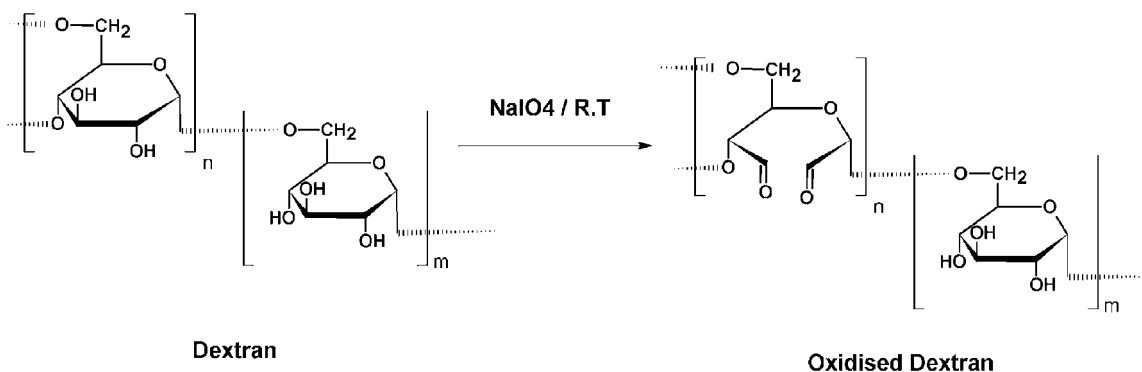
Sample	Zeta potential (mV)
Dex@AuNPs	−42.3
ABA@AuNPs	−33.3
RBITC@AuNPs	−11.2

the surrounding of the nanoparticles due to the chemisorption of aminophenyl boronic acid by imine/Schiff's base formation as well as an increase in size. No significant broadening of the plasmon absorption spectra was observed after this step indicating that ABA@AuNPs did not experience any aggregation upon the conjugation of aminophenyl boronic acid. RBITC was adsorbed on the ABA@AuNPs by hydrogen bonding and it is resulted further red shift of SPR absorption to 544 nm with slight broadening.

Dynamic light scattering results showed that the Dex@AuNPs was composed of mono dispersed nanoparticles of 7 nm in size (Fig. 2). The TEM images of the particles after each modification are shown in Fig. 3 and indicate that the particles are spherical and well dispersed. TEM image of dually functionalized AuNPs is shown in Fig. 3C.

The results were further confirmed by ζ potential measurements. ζ potential was found to be less negative compared to Dex@AuNPs as a result of modification (Table 1). The surface of Dex@AuNPs enriched by boronic acid moieties and RBITC were also confirmed by FTIR analysis (Fig. 4). The FTIR spectrum of Dex@AuNPs showed peak around 1734 cm^{-1} , which corresponds to the $\text{C}=\text{O}$ stretching frequency, indicating the presence of active aldehyde groups on the surface. Two sharp peaks at 2925 cm^{-1} and 3355 cm^{-1} were attributed to $\text{C}-\text{H}$ and $\text{O}-\text{H}$ stretching bands of dextran on the AuNPs surface. Fig. 3B shows the FTIR spectrum of ABA@AuNPs with RBITC. The increase in peak intensity, compared to Fig. 4A around 1733 cm^{-1} was attributed to the combined effect of $\text{C}=\text{O}$ stretching frequency of carboxylic acid group in RBITC and free aldehyde group in activated dextran on the surface of Dex@AuNPs. Band at 1511 cm^{-1} corresponds to $\text{C}-\text{N}$ stretching of the reduced Schiff's base formed by the chemisorptions of aminophenyl boronic acid. The peak at 1336 cm^{-1} characteristic of $-\text{B}-\text{OH}$ stretching frequency confirms the presence of boronic acid moieties on the surface of Dex@AuNPs. The peak at 1653 cm^{-1} in Fig. 4A and 1644 cm^{-1} in Fig. 4B corresponds to $\text{O}-\text{H}$ bending frequency of unchanged hydroxyl group on the surface of Dex@AuNPs before and after modification.

The fluorescence spectra of pure RBITC and RBITC@AuNPs are shown in Fig. 5. RBITC exhibited a strong fluorescence peak at 594 nm in the aqueous solution of synthetic tear fluid (Fig. 5A). Interestingly, the fluorescence of RBITC adsorbed onto the AuNPs (RBITC@AuNPs) is significantly reduced (Fig. 5B). The fluorescence intensity came down to 13 AU from 800 AU. AuNPs are known



Scheme 1. Periodate oxidation of dextran.

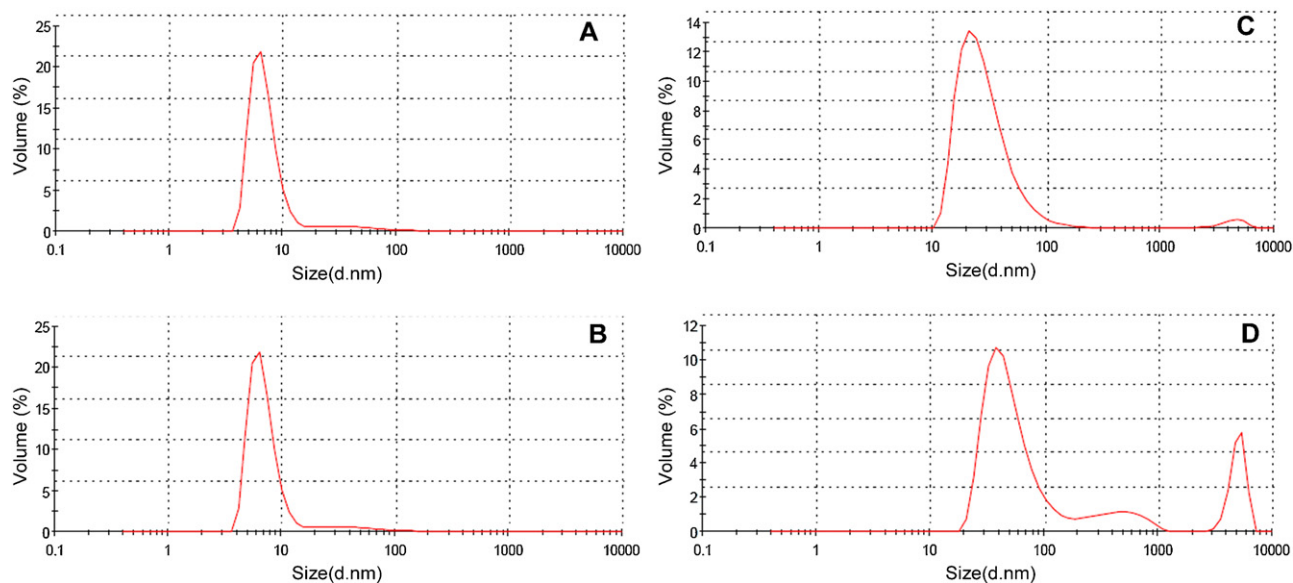


Fig. 2. DLS data of AuNPs at different stages of modification, (A) Dex@AuNPs, (B) AB A@AuNPs, (C) RBITC@AuNPs and (D) RBITC@AuNPs after equilibrating with 0.138 μM glucose.

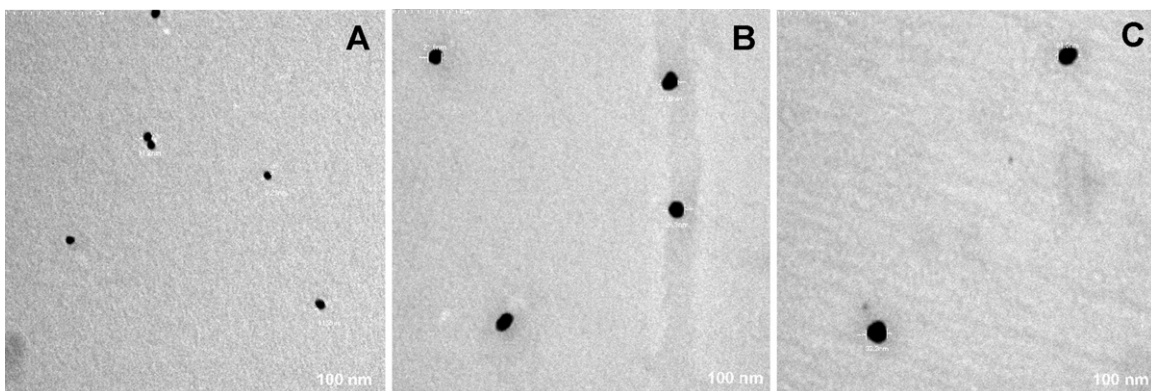


Fig. 3. TEM images at different stages of modification, (A) Dex@AuNPs, (B) AB A@AuNPs and (C) RBITC@AuNPs.

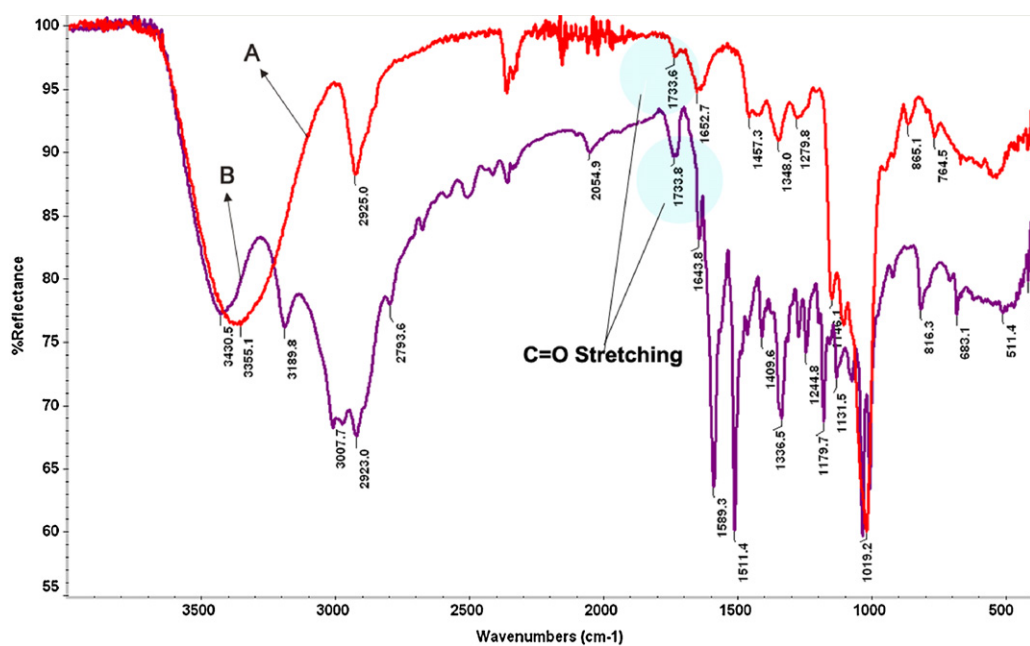


Fig. 4. FTIR spectra of (A) Dex@AuNPs and (B) RBITC@AuNPs.

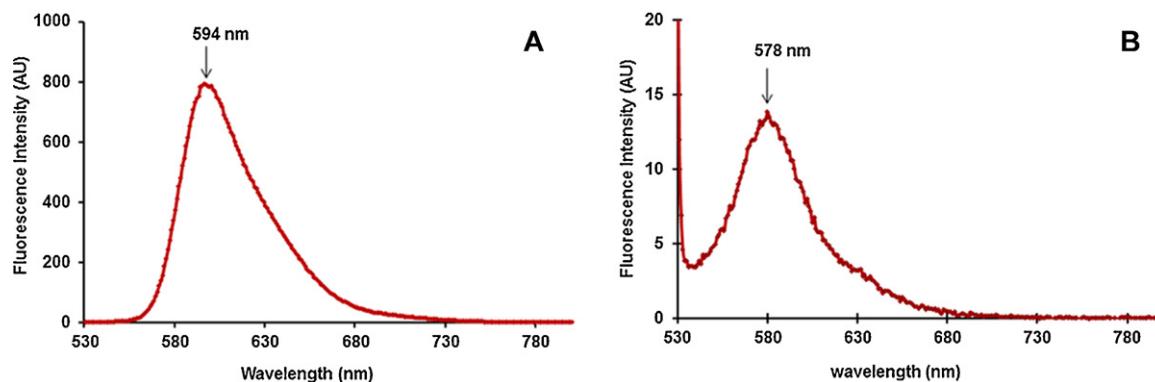


Fig. 5. Fluorescence spectra of RBITC and RBITC@AuNPs. The emission is almost quenched by the AuNPs (from 800 AU, the intensity scaled down to 13 AU).

as excellent quenchers either by a FRET (fluorescence resonance energy transfer) or electron transfer type mechanism [33]. It can be seen that, in RBITC@AuNPs, the peak of RBITC is blue shifted from 594 nm to 578 nm. Fluorescence peak is known to be blue shifted when the fluorophore moves to a hydrophobic pocket [34]. We feel that, blue shift in the emission, is due to more hydrophobic environment experienced by the fluorophore adsorbed on to the modified nanoparticles. The hydrophobic environment of the fluorophore is expected to enhance since it is more close to the aromatic moiety of the aminophenyl boronic acid.

The fluorescence spectra of RBITC@AuNPs after equilibration in solution containing varied amount of glucose is shown in Fig. 6A.

The drastically reduced fluorescence was found to revive with the addition of glucose to the solution of RBITC@AuNPs. The fluorescence intensity was increased with increase in glucose concentration. We plotted the change in fluorescence intensity versus the concentration of the glucose. The graph (Fig. 6B) shows a proportional fluorescence increase with the increase in concentration

of glucose. One interesting feature is the leveling off the changes in fluorescence once the concentration of glucose exceeded $0.138 \mu\text{M}$. Beyond this concentration, the fluorescence intensity remained constant presumably an indication of the saturation of the available boronic acid moieties on the surface of particles. We observed a linear change in the fluorescence with increase in glucose concentration and we considered $0.005 \mu\text{M}$ as the detection limit of this fluorescence sensor system.

We presumed that in the system, fluorophore (RBITC) is surrounded by phenyl boronic acids moieties possibly through hydrophobic interaction between the aromatic rings and hydrogen bonding between boronic acid groups and the carboxyl groups in the fluorophore. It is reasoned that at pH 7.4, boronic acid moieties exist in its trigonal neutral form [35]. Since glucose has a strong affinity towards boronic acid moiety, competitive binding take place with the formation of reversible covalent bond with hydroxyl group of glucose. Formation of glucose-boronate ester shifts the acid-base equilibrium of the boronic acid towards its

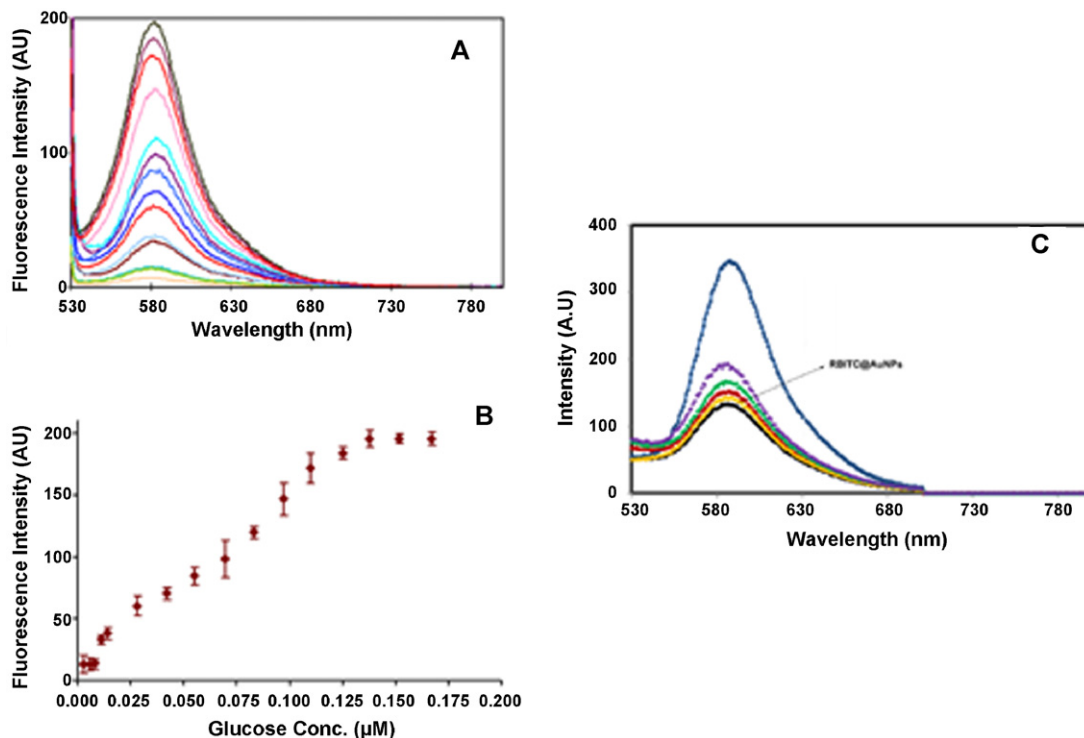


Fig. 6. (A) The revival of the fluorescence of RBITC@AuNPs in the presence of glucose, (B) shows the graphical representation of fluorescence intensity versus concentration of glucose and (C) The increase in fluorescence of RBITC@AuNPs in the presence of glucose in real tear fluids collected from female adults (25–30 age group).

anionic tetrahedral “-ate” form [36]. The fluorescence intensity was found to increase when glucose molecules bind onto the boronic acid groups. This observation was attributed to the detachment of fluorophore from ABA@AuNPs by glucose binding. It is well known that there should be a minimum distance between AuNPs and the fluorophore to produce effective fluorescence quenching. In the presence of glucose, aggregation of particles leads to enhanced size and as a result the distance between RBITC and AuNPs is increased. The significant broadening of plasmon absorption peak (Fig. 1D) apparently reflects increase in size of the particles on the onset of glucose binding. Additionally, repulsion between the anionic boronic acid of the complex and the -COO^- (the probability of ionization of -COOH groups of the fluorophore to form -COO^- ions is more at a pH of 7.4) groups in RBITC may also be causative to detach the fluorophore from the surface of the nanoparticles. Recently Wu et al. have shown glucose mediated assembly of phenylboronic acid (PBA) modified quantum dots [37]. They have shown an increase in size of the PBA-quantum dots assembly with an increase in glucose concentration. To get a view how glucose influence the morphology of the particles, we analyzed the modified particles prior and after glucose binding. The DLS data is shown in Fig. 2. As indicated in trace 2A, hydrodynamic volume of Dex@AuNPs is around 7 nm, [PDI=0.487]. The size of AuNPs after modification with aminophenyl boronic acid followed by RBITC is increased to 26.31 [PDI=0.487] and 30.68 nm [PDI=0.424] respectively (Fig. 2B and C). A typical trace of the RBITC@AuNPs after incubating with glucose is shown in Fig. 2D. Size of the particles is increased to 104 nm [PDI=0.675] reflecting remarkable swelling as a result of glucose binding. DLS traces conclusively suggest that the increase in fluorescence intensity with respect to the concentration of glucose is indeed due to the enhanced distance between AuNP and fluorophore acquired by glucose induced swelling. Additionally, plasmon absorption of particles in the presence of glucose is also broadened and red shifted significantly further reflecting the increase in size (trace D in Fig. 1).

Tear glucose level is about 5–10 fold less than the concentration of glucose in the blood depending upon the type of diabetics and its severity. Srivastav et al. [38] compared the glucose concentration in blood and in tear fluid. They showed that average glucose range of tear fluid in diabetes is 5–12 mg/dL (27.7–66.7 μM) during fasting and 15–22 mg/dL (83.3–122.2 μM) during postprandial. It seems that the methodology reported here has adequate sensitivity to detect glucose in tear. Earlier studies have shown good selectivity of PBA modified probes towards glucose pointing out its suitability in the continuous monitoring of glucose [39–42]. It is known that tear is free from other sugars and glucose monitoring in tear thereby is simpler since intervention from normal interfering molecules in blood glucose analysis is absent. The method discussed here is very sensitive and required sample (tear fluid) volume can be limited to few μL . To substantiate this view, we analyzed real tear fluids collected from healthy human volunteers as depicted in Section 2.1.8. The fluorescence traces of RBITC@AuNPs in the presence of human tear fluid are shown in Fig. 6C. Sample collected from each individual showed varied emission intensity reflecting the varied level of glucose in those fluids. We quantified glucose in these samples using the graph generated from fluorescence spectra obtained using standards (Fig. 6A). The trace shown maximum intensity in Fig. 6C was omitted for quantification since that sample was little turbid. The remaining four tear samples showed a glucose level of 0.087 μM , 0.095 μM , 0.11 μM and 0.125 μM respectively. These concentrations fall in the same range of normal values of glucose in tear fluids reported earlier [43]. The measurement of glucose in tear fluids show that the present method has enough potential to develop further as a simple, rapid and sensitive methodology to monitor glucose without drawing blood.

4. Conclusion

In the present study we demonstrated a simple and sensitive approach for the detection and estimation of glucose in aqueous fluids (e.g. synthetic tear) using dually functionalized AuNPs. The AuNPs were generated using mildly oxidized dextran and aminophenyl boronic acid, a well known ligand for glucose, is conjugated through Schiff's base formation. Rhodamine B isocyanate was then adsorbed onto modified particles. The fluorescence of RBITC@AuNPs was found to increase concomitantly with glucose concentration and this observation was employed in the detection of glucose. Our approach is able to detect glucose concentrations from 0.025 μM to 0.125 μM , ideal for glucose monitoring in tear fluid in which the glucose concentration is very low. The analysis can be performed with small volumes which is again suitable for tear analysis since at a time only low volume sample can be drawn. The potential application of the method is demonstrated by assessing real tear samples taken from healthy human volunteers. The glucose concentrations in these fluids agreed well with values reported earlier in tear fluids of human beings.

Acknowledgments

The authors wish to thank CSIR and DBT, New Delhi, India for financial support.

References

- [1] B. Rabinovitch, W.F. March, R.L. Adams, *Diabetes Care* 5 (1982) 254–258.
- [2] I.J. Hatoum, F.B. Hu, J.J. Nelson, E.B. Rimm, *Diabetes* 59 (2010) 1239–1243.
- [3] A.N. Kollias, M.U. Ulbig, *Dtsch. Arztebl. Int.* 107 (2010) 75–84.
- [4] T.A. Elasy, *Clin. Diabetes* 28 (2010) 97–98.
- [5] A.H. Salanitro, C.L. Roumie, *Clin. Diabetes* 28 (2010) 107–114.
- [6] M.R. Robinson, R.P. Eaton, D.M. Haaland, G.W. Koepp, E.V. Thomas, B.R. Stallard, P.L. Robinson, *Clin. Chem.* 38 (1992) 1618–1620.
- [7] E.P. Sander, S.S. Odell, K.K. Hood, *Diabetes Spectrum* 23 (2010) 89–94.
- [8] J.D. Lane, D.M. Krumholz, R.A. Sackb, C. Morris, *Curr. Eye Res.* 31 (2006) 895–901.
- [9] V.L. Alexeev, S. Das, D.N. Finegold, S.A. Asher, *Clin. Chem.* 50 (2004) 2353–2360.
- [10] D.K. Bishop, J.T. La Belle, S.R. Vossler, D.R. Patel, C.B. Cook, J. *Diabetes Sci. Technol.* 4 (2010) 299–306.
- [11] R. Badugu, J.R. Lakowicz, C.D. Geddes, *Journal of Fluoresc.* 14 (2004) 371–374.
- [12] C.R. Taormina, J.T. Baca, D.N. Finegold, S.A. Asher, J.J. Grabowski, *J. Am. Soc. Mass Spectrom.* 18 (2007) 332–336.
- [13] K. Aslan, J.R. Lakowicz, C.D. Geddes, *Anal. Biochem.* 330 (2004) 145–155.
- [14] H. Liu, D. Chen, L. Yang, X. Ren, F. Tang, J. Ren, *Nanotechnology* 21 (2010) 185504–185510.
- [15] S. Lee, V.H. Perez-Luna, *Anal. Chem.* 77 (2005) 7204–7211.
- [16] F.W. Campbell, R.G. Compton, *Anal. Bioanal. Chem.* 396 (2009) 241–259.
- [17] S. Chah, M.R. Hammond, R.N. Zare, *Chem. Biol.* 12 (2005) 323–328.
- [18] A.T. Gates, S.O. Fakayode, M. Lowry, G.M. Ganea, A. Murugesu, J.W. Robinson, R.M. Strongin, I.M. Warner, *Langmuir* 24 (2008) 4107–4113.
- [19] D. Astruc, M.C. Daniel, J. Ruiz, *Chem. Commun.* 15 (2004) 2637–2649.
- [20] P. Baptista, E. Pereira, P. Eaton, G. Doria, A. Miranda, I. Gomes, P. Quaresma, R. Franco, *Anal. Bioanal. Chem.* 391 (2008) 943–950.
- [21] L.J. Fan, Y. Zhang, W.E. Jones, *Macromolecules* 38 (2005) 2844–2849.
- [22] I.B. Kim, U.H.F. Bunz, *J. Am. Chem. Soc.* 128 (2006) 2818–2819.
- [23] C.C. Huang, H.T. Chang, *Anal. Chem.* 78 (2006) 8332–8338.
- [24] C.J. Mu, D.A. LaVan, R.S. Langer, B.R. Zetter, *ACS Nano* 4 (2010) 1511–1520.
- [25] F. Cannone, G. Chirico, *J. Phys. Chem. B* 110 (2006) 16491–16498.
- [26] S.Y. Lim, J.H. Kim, J.S. Lee, C.B. Park, *Langmuir* 23 (2009) 13302–13305.
- [27] T. Huang, R.W. Murray, *Langmuir* 18 (2002) 7077–7081.
- [28] B. Dubertret, M. Calame, A.J. Libchaber, *Nat. Biotechnol.* 19 (2001) 365–370.
- [29] A. Jeanes, C.A. Wilham, *J. Am. Chem. Soc.* 72 (1950) 2655–2657.
- [30] M. Sokolsky-Papkov, J. Abraham, A.J. Domb, J. Golenser, *Biomacromolecules* 7 (2006) 1529–1535.
- [31] S. Lee, H. Victor, P. Luna, *Anal. Chem.* 77 (2005) 7204–7211.
- [32] S. Nath, C. Kaftanis, A. Tinkham, J.M. Perez, *Anal. Chem.* 80 (2008) 1033–1038.
- [33] U.H.F. Bunz, V.M. Rotello, *Angew. Chem. Int. Ed.* 49 (2010) 3268–3279.
- [34] G.A. Caputo, E. London, *Biochemistry* 42 (2003) 3275–3285.
- [35] Y. Nambu, K. Yamamoto, T.J. Endo, *Chem. Soc. Commun.* 7 (1986) 574–575.
- [36] D.B. Cordes, S. Gamsey, B. Singaram, *Angew. Chem. Int. Ed.* 45 (2006) 3829–3832.
- [37] W. Wu, T. Zhou, A. Berliner, P. Banerjee, S. Zhou, *Angew. Chem. Int. Ed.* 49 (2010) 1–6.

- [38] G.R. Srivastav, B.K. Jain, R. Sahai, A. Sharma, S. Verma, *Proc. AIOC* (2006) 302–305.
- [39] A.P. Davis, R.S. Wareham, *Angew. Chem. Int. Ed.* 38 (1999) 2978–2982.
- [40] M.M.M. Muscatello, L.E. Stunia, S.A. Asher, *Anal. Chem.* 81 (2009) 4978–4985.
- [41] A. Kabilan, A.J. Marshall, F.K. Sartain, M.C. Lee, A. Hussain, X. Yang, J. Blyth, N. Karangu, K. James, J. Zeng, D. Smith, A. Domschike, C.R. Lowe, *Biosens. Bioelectron.* 20 (2005) 1602–1609.
- [42] W. Wu, T. Zhou, S. Zhou, *Chem. Commun.* (2009) 4390–4391.
- [43] K.M. Daum, R.M. Hile, *Invest. Ophthalmol. Vis. Sci.* 22 (1982) 509–514.